

Spectral diffusion induced by energy transfer in doped organic glasses: Delay-time dependence of spectral holes

F. T. H. den Hartog and C. van Papendrecht^{a)}

Center for the Study of Excited States of Molecules, Huygens and Gorlaeus Laboratories, University of Leiden, P.O. Box 9504, 2300 RA Leiden, The Netherlands

R. J. Silbey

Department of Chemistry, Massachusetts Institute of Technology, Cambridge, Massachusetts 02139

S. Völker^{b)}

Center for the Study of Excited States of Molecules, Huygens and Gorlaeus Laboratories, University of Leiden, P.O. Box 9504, 2300 RA Leiden, The Netherlands

(Received 27 July 1998; accepted 2 October 1998)

A new effect in doped organic glasses, which we refer to as “energy transfer (ET)-induced spectral diffusion (SD),” ET→SD, has recently been reported by us. In this process “extra” SD, in addition to “normal” SD in glasses, is triggered by the energy balance released on “downhill” ET. Quantitative aspects of the ET→SD process have been investigated by means of time-resolved hole-burning experiments on free-base chlorin (H₂Ch) in polystyrene (PS) presented here. The “effective” homogeneous linewidth Γ'_{hom} was determined as a function of delay time t_d (10^{-5} – 10^3 s), temperature (1.2 to 4.2 K) and concentration ($c=1\times 10^{-5}$ to 6×10^3 M), at various excitation wavelengths within the $S_1\leftarrow S_0$ 0-0 band. Γ'_{hom} as a function of temperature was found to obey the relation $\Gamma'_{\text{hom}}=\Gamma'_0+aT^{1.3}$, characteristic for glasses, and we present an analysis of the residual linewidth Γ'_0 and the coupling constant a . In this analysis we determined (i) the separate contributions to Γ'_0 arising from the fluorescence lifetime, ET, and ET→SD, (ii) the separate contributions to a arising from “pure” dephasing, “normal” SD, and “extra” spectral diffusion caused by ET→SD. The contributions of ET→SD to Γ'_0 and a prove to be proportional to the concentration and to the logarithm of the delay time ($\propto c \log t_d$). © 1999 American Institute of Physics. [S0021-9606(99)53001-8]

I. INTRODUCTION

While studying the effect of energy transfer and concentration on optical dephasing in doped organic glasses at low temperature by hole-burning,¹ we discovered that the “effective” homogeneous linewidth Γ'_{hom} was much larger than expected on the basis of a simple Förster mechanism and that there must be an extra contribution to spectral diffusion. We called this new effect “energy transfer-induced spectral diffusion,” ET→SD.² The key question to understand is: how do we distinguish hole broadening due to a reduction of T_1 by “downhill” energy transfer from hole broadening due to spectral diffusion? Surprisingly, this problem had not previously been addressed, although broadening of holes with concentration and excitation energy had been reported and attributed to energy transfer, without being quantitatively analyzed.^{3,4}

To recognize whether the holewidth, or the “effective” homogeneous linewidth Γ'_{hom} , was determined by a direct energy transfer process of the Förster type⁵ or by some other process, we looked for changes occurring in Γ'_{hom} when varying the excitation wavelength λ_{exc} over the 0-0 band and the concentration c .² We studied the $S_1\leftarrow S_0$ 0-0 transition of

free-base chlorin (H₂Ch) in polystyrene (PS). A prerequisite for Förster’s “downhill” energy transfer (ET) is an overlap between the fluorescence spectrum of the donor and the absorption spectrum of the acceptor. In the system H₂Ch in PS, the donor and acceptor molecules are chemically identical and the spectral overlap is given through the broad phonon side-bands centered at $\Delta E\approx 20$ to 40 cm^{-1} from the narrow zero-phonon line. The ET-rate and, therefore, the holewidth related to the (donor) molecules burnt at λ_{exc} would then be determined by the number of (acceptor) molecules which have their zero-phonon transitions approximately $2\Delta E$ lower in energy. Since the number of molecules at a given wavelength is proportional to the intensity of the inhomogeneous absorption band (a Gaussian curve), the effect of direct “downhill” energy transfer on Γ'_{hom} will depend on λ_{exc} in such a way that the largest value of Γ'_{hom} would be found at $\sim 40\text{--}80\text{ cm}^{-1}$ to the blue of the maximum of the inhomogeneous absorption band. Thus, if “downhill” ET would determine the value of Γ'_{hom} , the λ_{exc} -dependence of Γ'_{hom} would follow the profile of the 0-0 band with a slight blue-shift.

But, if ET also influences the dynamics of the glass by dumping part of the “heat” released during the ET-process into the TLSs, then not only the primary step in the ET-process will affect the TLSs, but also subsequent transfer steps involving molecules absorbing all the way to the red

^{a)}Present address: Netherlands Measuring Institute, P.O. Box 654, 2600 AR Delft, The Netherlands.

^{b)}To whom correspondence should be addressed.

edge of the 0-0 band will contribute to an increase of Γ'_{hom} . Under these conditions, Γ'_{hom} will be proportional to the total number of molecules absorbing to the red of λ_{exc} and, thus, will increase continuously from the red to the blue of the inhomogeneous 0-0 band, leveling off at the blue edge.

In our previous study of the effect of ET on Γ'_{hom} (Ref. 2) we have found that Γ'_{hom} follows an S-shaped curve as a function of λ_{exc} , the amplitude of the curve increasing with concentration. Since the S-shaped curves could be fitted with an error function found to coincide with the normalized area of the 0-0 band at wavelengths longer than λ_{exc} , we concluded that Γ'_{hom} was not directly, but indirectly determined by “downhill” ET.

By increasing the concentration c , the amount of ET increases. Direct energy transfer implies that Γ'_{hom} increases proportionally with c^2 ,⁶⁻⁸ but we have found $\Gamma'_{\text{hom}} \propto c$.² Furthermore, Förster’s mechanism predicts that the ET-rate is proportional to $(R_0/R)^6$, where $R_0 \approx 30-80 \text{ \AA}$ is the critical Förster radius or distance between donors and acceptors for which the transfer rate is equal to the rate of fluorescence decay, and R is the donor-acceptor distance. If Γ'_{hom} measured in Ref. 2 were determined by Γ_0^{ET} , one would obtain values of R_0 far in excess of a reasonable Förster radius. Finally, from the ET-mechanism one would also expect more sharply peaked line shapes than Lorentzians, contrary to what we found. Thus, our results obtained for Γ'_{hom} point to a multi-step process involving all molecules absorbing towards the red of λ_{exc} .

The clearest indication that the TLS-dynamics is affected by “downhill” ET would be an increase of Γ'_{hom} with t_d (the time between burning and probing) over many orders of magnitude in time that becomes the more pronounced the higher the concentration. Since all ET-steps are over during the fluorescence lifetime of the chromophore ($\tau_{\text{fl}} = 8 \text{ ns}$ for H_2Ch), an increase of Γ'_{hom} observed at delay times $t_d > \tau_{\text{fl}}$ must be due to a change in the TLS-dynamics. We have indeed verified that Γ'_{hom} increases with delay time and concentration, even at temperature $T \rightarrow 0$.² Apparently, “heat” is stored in the TLSs during the short-time “downhill” ET-process. The activated TLSs will relax over a long period of time and give rise to long-term spectral diffusion. The difference between this “extra” SD and “normal” SD in glasses is that the latter vanishes for $T \rightarrow 0$. If the ET \rightarrow SD mechanism that we have proposed in Ref. 2 is correct, one would expect that “extra” SD could also be induced by dumping infrared radiation of a few cm^{-1} to hundreds of cm^{-1} directly into the glass doped at low concentrations, i.e., in the absence of ET. Such an experiment has still to be done.

In this paper we present a quantitative experimental analysis of the ET \rightarrow SD mechanism. Time-resolved hole-burning has been performed on the glassy system H_2Ch in PS at concentrations c between 10^{-5} and $6 \times 10^{-3} \text{ M}$, and Γ'_{hom} has been determined as a function of delay time t_d between 10^{-5} and 10^3 s and temperature T from 1.2 to 4.2 K, in both the red and the blue wing of the $S_1 \leftarrow S_0$ 0-0 band. From the results we obtain the separate contributions of the fluorescence lifetime τ_{fl} , “pure” dephasing, “normal”

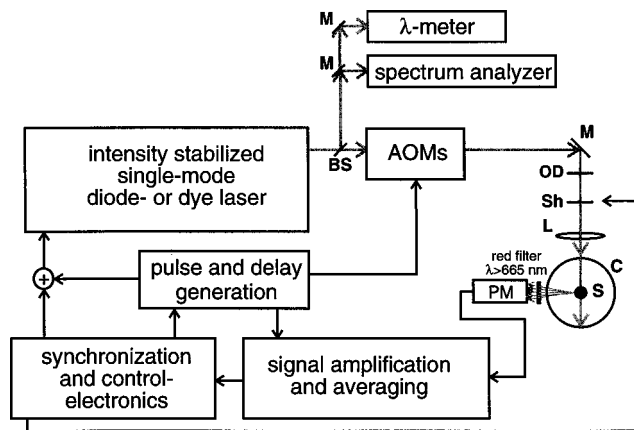


FIG. 1. Schematic representation of the experimental arrangement used for time-resolved HB. The holes were burnt either with a tunable *cw* single-frequency dye-laser pumped by an Ar^+ -laser or with a temperature- and current-controlled single-mode diode-laser. The holes were detected, after a variable delay, in fluorescence excitation. λ -meter: Michelson-type interferometer, M: mirror, BS: beamsplitter, OD: optical density filter, Sh: shutter, L: lens, C: cryostat, S: sample, PM: photomultiplier.

spectral diffusion, “downhill” ET and ET \rightarrow SD to Γ'_{hom} , together with their functional dependences on c and t_d .

II. EXPERIMENTAL METHODS

Free-base chlorin (H_2Ch) was prepared as described in Refs. 2, 9 and incorporated in polystyrene (PS) films.² The samples were placed in a home-built ^4He cryostat, the temperature of which was controlled by the helium vapor pressure and measured with a calibrated carbon resistor in contact with the sample, with an accuracy better than 0.01 K.

Time-resolved spectral hole-burning (HB) experiments were performed by applying a sequence of three laser pulses.^{10,11} During the first pulse the frequency of the laser is scanned over the part of the inhomogeneous absorption band of interest in order to obtain a base line. The second pulse, which creates the hole, is applied at a fixed frequency and higher laser intensity than the first one. The hole is probed after a variable delay time t_d with a third pulse at low intensity. During the third pulse the frequency of the laser is scanned over the same part of the absorption band as during the first pulse. The delay time t_d between burning and probing the hole was varied between 10^{-5} and 10^3 s .

A schematic representation of the experimental set-up is shown in Fig. 1. Two types of *cw* single-mode lasers were used, depending on the time scale of the experiment. For delay times shorter than 200 ms, we used a current- and temperature-controlled diode laser (Hitachi HL 6312G, $P_{\text{max}} = 5 \text{ mW}$, $632 < \lambda < 638 \text{ nm}$, bandwidth $\Gamma_{\text{laser}} \approx 30 \text{ MHz}$). The frequency scan speed of this diode laser is $\sim 0.5 \text{ GHz}/\mu\text{s}$. For delay times longer than 200 ms, a dye laser (Coherent 599-21 with intracavity assembly, $\Gamma_{\text{laser}} \approx 2 \text{ MHz}$, dye DCM) pumped by an Ar^+ -laser (Spectra Physics 2030-15) was used. The intensity of the laser light was stabilized by a home-built active stabilization circuit with an accuracy better than 0.5%. The frequency scan speed of the dye laser is limited to $\sim 100 \text{ MHz/ms}$ by piezo-

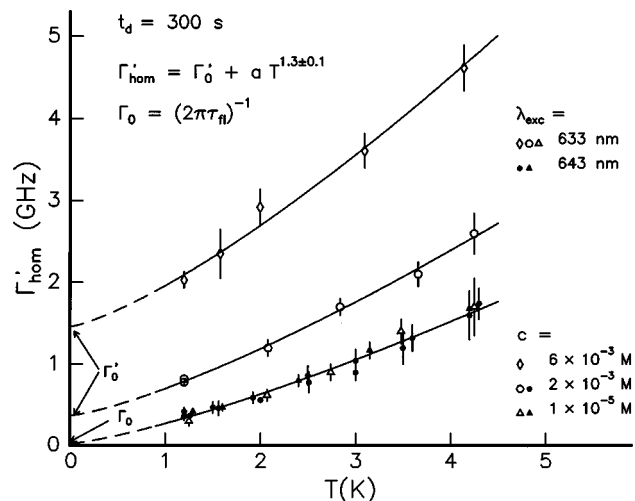


FIG. 2. Temperature dependence of Γ'_{hom} of the $S_1 \leftarrow S_0$ 0-0 transition of H_2Ch in PS for three concentrations, in the blue ($\lambda_{\text{exc}} = 633$ nm) and red wings ($\lambda_{\text{exc}} = 643$ nm), for $t_d = 300$ s. Γ'_{hom} and Γ_0 increase with concentration and towards the blue. The three curves follow a $T^{1.3}$ -power law.

electronically driven mirrors; this speed is about 10^4 times slower than that of the diode laser. The wavelength of the lasers was calibrated with a Michelson interferometer (home-built, resolution ~ 50 MHz), and its mode structure was monitored with a confocal Fabry-Perot étalon.

The burn and probe pulses were generated as described in Refs. 10–12. A shutter blocked the beam in front of the cryostat before and after the experiment. The laser beam was focussed on the sample to an area $A \approx 0.03$ cm 2 . Burning-power densities from $P/A \sim 100$ nW/cm 2 to ~ 100 mW/cm 2 were used, with burning times varying from $t_b = 10$ μs to ~ 30 s. Thus, burning-fluence densities varied between $Pt_b/A \sim 50$ $\mu\text{J}/\text{cm}^2$ and ~ 10 J/cm 2 .

The holes were detected in fluorescence excitation with a cooled photomultiplier (PM, EMI 9658R). To separate the fluorescence signal from the scattered laser light, a few long-wavelength pass filters were used (Schott RG665, total thickness ~ 1.5 cm) such that $\lambda_{\text{det}} \geq 665$ nm. For delay times shorter than 30 s, the signal from the PM was amplified with a load resistor and a differential preamplifier (HMS-Elektronik, model 568) or a bandpass amplifier (Ithaco, model 1201). For delay times longer than 30 s, the signal from the PM was amplified with an electrometer (Keithley, model 610 C). The signals were averaged in different ways, depending on delay time. For delay times shorter than 30 s, a sequence of probe-burn-probe cycles was applied with an appropriate repetition rate ≤ 10 Hz. After each probe-burn-probe cycle, the frequency of the laser was slightly shifted (about twice the holewidth) to obtain a fresh baseline for each hole burnt. Transient holes, which live about 2 ms (see below), were averaged 10^3 to 10^4 times. For persistent holes with 2 ms $\leq t_d \leq 30$ s, the signals were averaged 50 to 100 times with a digital oscilloscope (LeCroy 9310 or 9360, both with bandwidth 300 MHz, or LeCroy 9410 with bandwidth 150 MHz). If longer averaging were used, the signal of the baseline region would decrease due to the presence of previously burnt holes. For delay time longer than 30 s, the holes were averaged point by point about 1000 times with the PC,

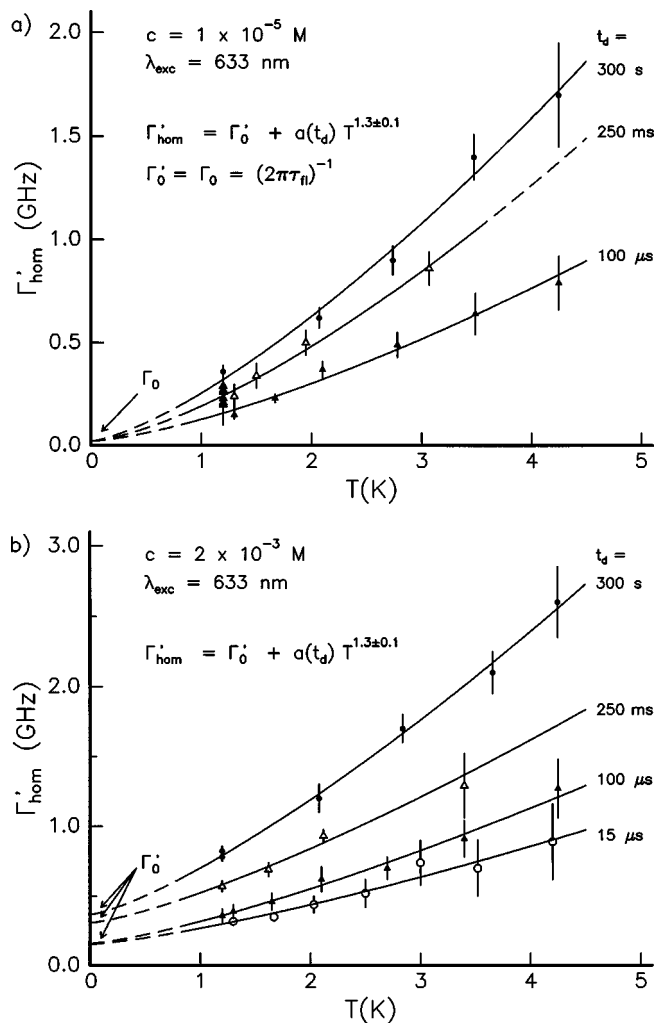


FIG. 3. (a) Temperature dependence of Γ'_{hom} at low concentration, for three delay times, in the blue wing. Γ'_{hom} extrapolates to $\Gamma_0 = \Gamma_0 = (2\pi\tau_{\text{fl}})^{-1} \sim 20$ MHz, with $\tau_{\text{fl}} \approx 8$ ns. (b) Temperature dependence of Γ'_{hom} at $c = 2 \times 10^{-3}$ M, for four delay times, in the blue wing. Γ_0 increases with t_d .

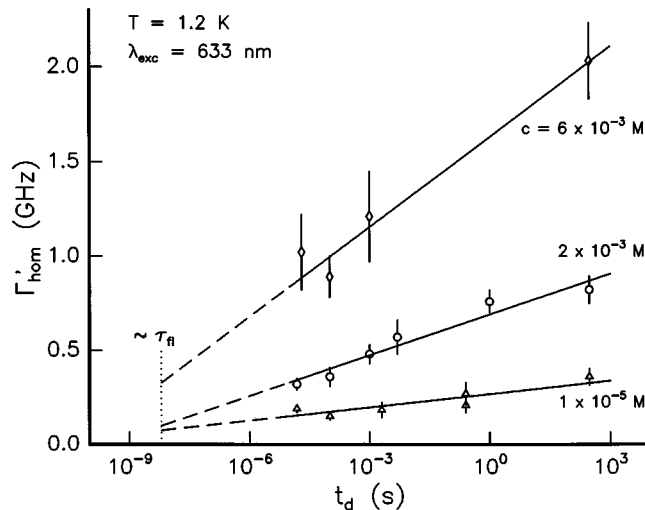


FIG. 4. Γ'_{hom} as a function of the logarithm of t_d at $T = 1.2$ K, for three concentrations, in the blue wing. The data follow $\Gamma'_{\text{hom}} \propto \log(t_d)$.

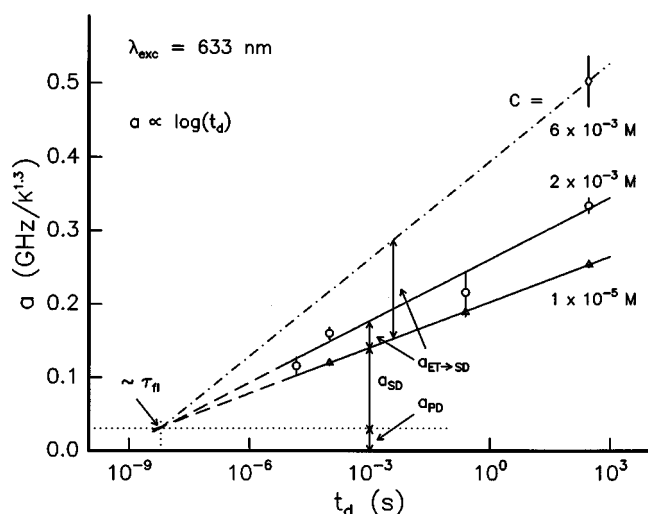


FIG. 5. Coupling constant a in Eq. (5) as a function of $\log(t_d)$ for three concentrations, at $\lambda_{\text{exc}} = 633$ nm. All lines intersect at $t_d \approx \tau_{\text{fl}}$. For $t_d < \tau_{\text{fl}}$ there is no SD, and only ‘‘pure’’ dephasing remains. The data follow $a \propto \log(t_d)$.

with a total number of ~ 300 points. The experiments were controlled with a personal computer.

Transient holes result from population storage in the triplet state. The lifetime of the triplet state of H_2Ch in PS, $\tau_{\text{triplet}} = (1.4 \pm 0.1)$ ms, was obtained by measuring the area of a transient hole as a function of delay time (not shown). The value of τ_{triplet} was found to be independent of concentration.

The ‘‘effective’’ homogeneous linewidth Γ'_{hom} at a delay time t_d was determined in the following way. The holes were measured at various burning-fluence densities Pt_b/A and their profile fitted with Lorentzian curves. The holewidths Γ_{hole} were then extrapolated to $\text{Pt}_b/A \rightarrow 0$ to take into account the effect of power broadening; this yields $\Gamma_{\text{hole},0}(t_b, t_d)$. For $t_d > t_b$,^{10,12}

$$\Gamma_{\text{hole},0}(t_b, t_d) = \Gamma'_{\text{hom}}(t_b) + \Gamma'_{\text{hom}}(t_d) + 2\Gamma_{\text{laser}}. \quad (1)$$

To determine $\Gamma'_{\text{hom}}(t_d)$, we first measure the holewidth at delay time $t_d = t_b$. Thus,

$$\Gamma_{\text{hole},0}(t_b, t_b) = 2\Gamma'_{\text{hom}}(t_b) + 2\Gamma_{\text{laser}}. \quad (2)$$

Inserting $\Gamma'_{\text{hom}}(t_b)$ from Eq. (2) into Eq. (1), yields

$$\Gamma'_{\text{hom}}(t_d) = \Gamma_{\text{hole},0}(t_b, t_d) - \frac{1}{2}\Gamma_{\text{hole},0}(t_b, t_b) - \Gamma_{\text{laser}}. \quad (3)$$

For $t_d > 30$ s, we have used Eq. (3). For $t_d < 30$ s, $t_b \approx t_d$ and Eq. (3) reduces to

$$\Gamma'_{\text{hom}}(t_d) = \frac{1}{2}\Gamma_{\text{hole},0}(t_b, t_b) - \Gamma_{\text{laser}}. \quad (4)$$

For experiments with the diode laser, $\Gamma_{\text{laser}} = 30$ MHz. For experiments with the dye-laser, where $\Gamma_{\text{laser}} \approx 2$ MHz, the last term in Eqs. (3) and (4) is negligible.

III. RESULTS AND DISCUSSION

To study quantitatively the various contributions to Γ'_{hom} in the presence of ‘‘downhill’’ energy transfer, we have performed a series of HB-experiments to be discussed in this section. Figure 2 shows the dependence of Γ'_{hom} on tempera-

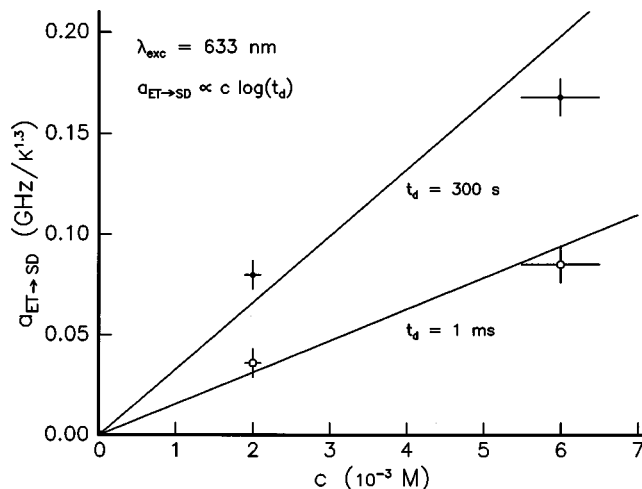


FIG. 6. The term $a_{\text{ET} \rightarrow \text{SD}}$ in Eq. (6) as a function of concentration. For $c = 1 \times 10^{-5}$ M, there is no ET and $a_{\text{ET} \rightarrow \text{SD}} = 0$. The data follow $a_{\text{ET} \rightarrow \text{SD}} \propto c \log(t_d)$.

ture for two excitation wavelengths within the 0-0 band and three concentrations, at a fixed delay time $t_d = 300$ s. The data points follow a power law characteristic for organic glasses at $T \leq 10$ K,^{10,11,13,14}

$$\Gamma'_{\text{hom}} = \Gamma'_0 + aT^{1.3 \pm 0.1}. \quad (5)$$

At the lowest concentration, the residual linewidth does not depend on excitation wavelength and is equal to $\Gamma_0 = (2\pi\tau_{\text{fl}})^{-1} \approx 20$ MHz, with $\tau_{\text{fl}} \approx 8$ ns the fluorescence lifetime of H_2Ch . At higher concentrations, $\Gamma'_0 = \Gamma_0$ only at the red-most wing of the 0-0 absorption band ($\lambda_{\text{exc}} = 643$ nm). Γ'_0 increases towards the blue and with increasing concentration.

As a consequence of ET \rightarrow SD, we concluded in Ref. 2 that Γ'_{hom} is expected to depend on delay time t_d , even at $T \rightarrow 0$. To distinguish ‘‘normal’’ SD from ‘‘extra’’ SD induced by ET, we performed the experiments shown in Figs. 3(a), 3(b) and Fig. 4. Figures 3(a) and 3(b) are plots of Γ'_{hom} vs temperature, for various delay times. For low concentrations [Fig. 3(a)], the value of Γ'_{hom} increases with delay time at a given temperature, and extrapolates to $\Gamma_0 = (2\pi\tau_{\text{fl}})^{-1}$, as expected for ‘‘normal’’ SD. For higher concentrations and in the blue wing of the band [Fig. 3(b)], however, Γ'_{hom} extrapolates to $\Gamma'_0 > \Gamma_0$, with Γ'_0 increasing with delay time, as expected from our ET \rightarrow SD mechanism.² Also Fig. 4, which is a plot of Γ'_{hom} vs the logarithm of t_d for three concentrations, measured in the blue wing of the band, supports the ET \rightarrow SD model. The data follow $\Gamma'_{\text{hom}} \propto \log(t_d)$, as for ‘‘normal’’ SD,^{10,15} but the slope $d\Gamma'_{\text{hom}}/d \log(t_d)$ increases with concentration. The results prove that the amount of ‘‘extra’’ SD is indeed enhanced by concentration and towards the blue part of the band. At the red onset of the band there is only ‘‘normal’’ SD, even at higher concentrations (not shown). From these results we conclude that ‘‘extra’’ SD is indeed triggered by ‘‘downhill’’ ET within the 0-0 band.

To assess the separate contributions to the coupling constant a in Eq. (5), we have plotted in Fig. 5 the value of a as a function of $\log(t_d)$. For $c = 1 \times 10^{-5}$ M and 2×10^{-3} M it was obtained from Figs. 3(a) and 3(b). Note that $a \propto \log(t_d)$

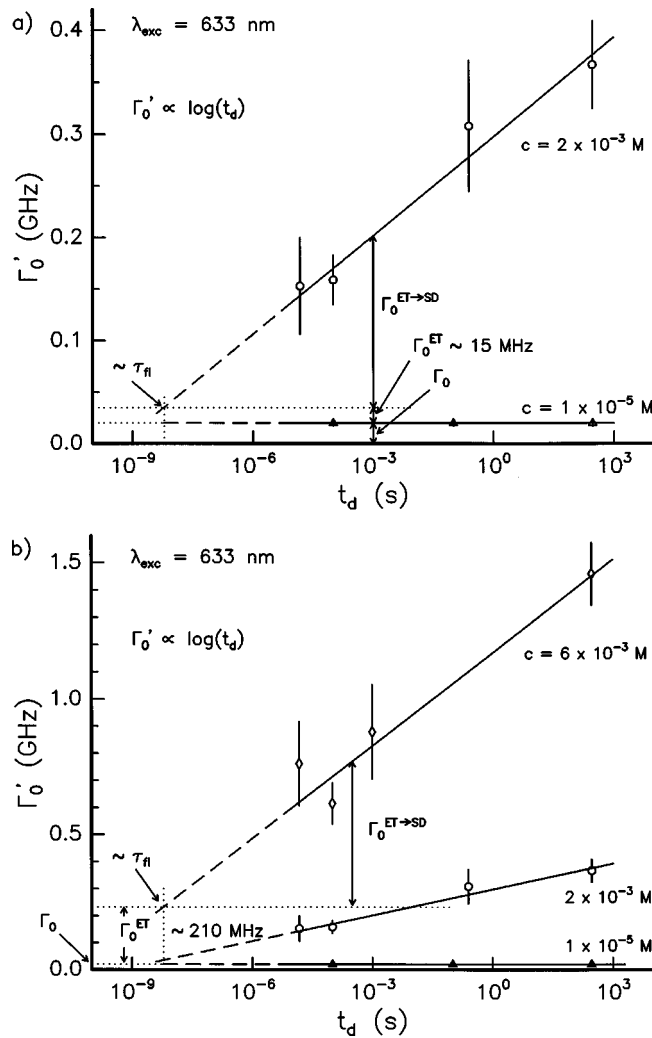


FIG. 7. (a) Residual linewidth Γ'_0 vs $\log(t_d)$, at $\lambda_{\text{exc}}=633$ nm. By extrapolating the upper curve to $t_d \approx \tau_{\text{fl}}$, the rate of direct energy transfer $\Gamma_0^{\text{ET}} \sim 15$ MHz for $c=2 \times 10^{-3}$ M is obtained. The data follow $\Gamma'_0 \propto \log(t_d)$. (b) Γ'_0 vs $\log(t_d)$, at $\lambda_{\text{exc}}=633$ nm, for three concentrations. The extrapolation of Γ'_0 to $t_d \approx \tau_{\text{fl}}$ yields $\Gamma_0^{\text{ET}} \sim 210$ MHz for $c=6 \times 10^{-3}$ M.

and the slope $da/d \log(t_d)$ increases with concentration. Furthermore, we observe that the two solid lines intersect at $t_d \approx \tau_{\text{fl}}$. If we assume that all values of a cross at this point, because there is no SD at $t_d < \tau_{\text{fl}}$,¹⁵ the value of a here should be given by a_{PD} , the contribution of ‘‘pure’’ dephasing. We find from Fig. 5 that $a_{\text{PD}}=(31 \pm 10)$ GHz/K^{1.3}. ‘‘Pure’’ dephasing arises from ‘‘fast’’ TLSs with relaxation rates R larger than $1/\tau_{\text{fl}}$. Since for $c=6 \times 10^{-3}$ M we only have a value of a at $t_d=300$ s (from Fig. 2), we have plotted this data point and traced a (broken) straight line from this point to the intersection of the other lines. Thus, a value of a for $c=6 \times 10^{-3}$ M at any delay time can be obtained from this line. The value of a for ‘‘normal’’ SD at any t_d can be obtained from the data at the lowest concentration. For this concentration, $a=a_{\text{PD}}+a_{\text{SD}}(t_d)$, with $a_{\text{SD}} \propto \log(t_d)$, as expected from the standard model TLS.^{15–18} The slope $da/d \log(t_d)=(21 \pm 1)$ MHz/K^{1.3} s at the lowest concentration and represents the amount of ‘‘normal’’ SD. For higher concentrations, the ‘‘extra’’ SD contribution $a_{\text{ET} \rightarrow \text{SD}}$ is then given by the difference between the value of a , at a given t_d

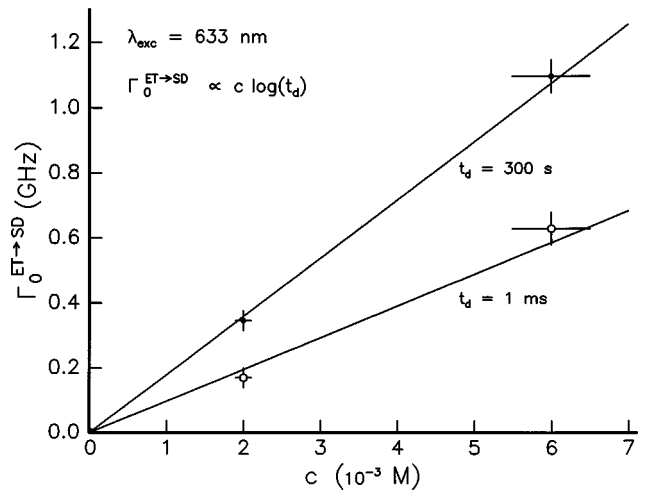


FIG. 8. The term $\Gamma_0^{\text{ET} \rightarrow \text{SD}}$ in Eq. (7) vs concentration, at $t_d=1$ ms and 300 s, for $\lambda_{\text{exc}}=633$ nm. The data points follow $\Gamma_0^{\text{ET} \rightarrow \text{SD}} \propto c \log(t_d)$.

for a specific concentration, and the value of $a_{\text{PD}}+a_{\text{SD}}(t_d)$ at $c=1 \times 10^{-5}$ M.

In Fig. 6, the contribution of ET \rightarrow SD to the coupling constant, $a_{\text{ET} \rightarrow \text{SD}}$, has been plotted as a function of concentration, for two delay times ($t_d=1$ ms and 300 s), in the blue wing. The data points follow an approximately linear dependence, from which we conclude

$$a_{\text{ET} \rightarrow \text{SD}} \propto c \log(t_d). \quad (6)$$

The separate contributions to the residual linewidth Γ'_0 , in the blue wing of the band, have been obtained from data as shown in Figs. 7(a), 7(b), and 8. Figures 7(a) and 7(b) are plots of Γ'_0 vs $\log(t_d)$. In Fig. 7(a) the data for $c=1 \times 10^{-5}$ and 2×10^{-3} M are displayed, whereas in Fig. 7(b) the data for 6×10^{-3} M are compared with those for the lower concentrations. The value of Γ'_0 in the absence of ET, $\Gamma_0=(2\pi\tau_{\text{fl}})^{-1}=20$ MHz, was obtained from the horizontal line for $c=1 \times 10^{-5}$ M. For $c=2 \times 10^{-3}$ M, Γ'_0 was obtained from Fig. 3(b), whereas for $c=6 \times 10^{-3}$ M, Γ'_0 was

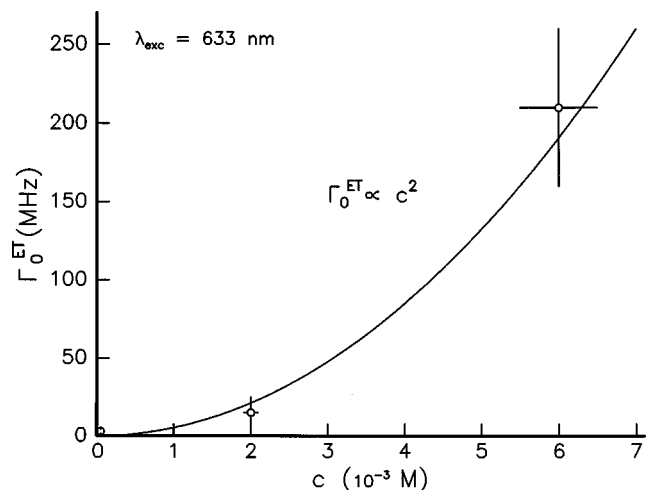


FIG. 9. The direct energy transfer term Γ_0^{ET} vs concentration, at $\lambda_{\text{exc}}=633$ nm. The data are consistent with Förster's energy transfer rate, $\Gamma_0^{\text{ET}} \propto c^2$.

taken from Fig. 2 and calculated from Fig. 5. The data follow $\Gamma'_0 \propto \log(t_d)$. By extrapolating the straight lines to $t_d \approx \tau_{fl}$, the contribution of SD is eliminated and the residual value of Γ'_0 at $t_d \approx \tau_{fl}$ is, therefore, the contribution of direct ET Γ_0^{ET} . We found $\Gamma_0^{ET} \approx 15$ MHz for $c = 2 \times 10^{-3}$ M [Fig. 7(a)] and $\Gamma_0^{ET} \approx 210$ MHz for $c = 6 \times 10^{-3}$ M [Fig. 7(b)]. By subtracting the value of $\Gamma_0 + \Gamma_0^{ET}$ at a given concentration from the value of Γ'_0 for this concentration and some given delay time t_d , we obtain $\Gamma_0^{ET \rightarrow SD}$ which increases linearly with $\log(t_d)$.

Figure 8 is a plot of $\Gamma_0^{ET \rightarrow SD}$ as a function of concentration, for two delay times ($t_d = 1$ ms and 300 s), in the blue wing. The values were obtained from Figs. 7(a) and 7(b). Since for $c = 1 \times 10^{-5}$ M there is no ET, $\Gamma_0^{ET \rightarrow SD} \approx 0$ for $c \rightarrow 0$. The data points appear to follow a straight line. Combining the results of Figs. 7 and 8, we conclude that

$$\Gamma_0^{ET \rightarrow SD} \propto c \log(t_d). \quad (7)$$

Finally, we have plotted the values of Γ_0^{ET} as a function of c , in the blue wing, in Fig. 9. Since at $c = 1 \times 10^{-5}$ M there is no ET, $\Gamma_0^{ET} = 0$. From Förster's mechanism for ET we expect $\Gamma_0^{ET} \propto c^2$.⁶⁻⁸ The data points in Fig. 9 are consistent with this expectation and, thus, we can estimate the values of Γ_0^{ET} for other concentrations of H₂Ch in PS from the figure. We note that the contribution of Γ_0^{ET} to Γ'_{hom} is small, even at the highest concentration ($\Gamma_0^{ET} \approx 0.25$ GHz vs $\Gamma'_{hom} \approx 2.5$ GHz for $c = 6 \times 10^{-3}$ M). If we now calculate the Förster radius $R_0 = R(\Gamma_0^{ET} \tau_{fl})^{1/6}$, where R is the average distance between the H₂Ch molecules, from the Γ_0^{ET} -values obtained for two concentrations, we get $R_0 = (67 \pm 1)$ Å. This value is within the range expected (30–80 Å) (Ref. 19) and supports the idea of our ET \rightarrow SD model.

IV. CONCLUSIONS

We have shown that the temperature-, concentration- and delay-time dependence of Γ'_{hom} of the 0-0 transition of H₂Ch in PS can consistently be described by taking into account “extra” SD indirectly induced by ET, in addition to direct energy transfer of the Förster's type and “normal” spectral diffusion.

Our results can be summarized as follows:

$$\Gamma'_{hom} = \Gamma'_0(c, \lambda_{exc}, t_d) + a(c, \lambda_{exc}, t_d) T^{1.3 \pm 0.1} \quad (8)$$

with

$$\Gamma'_0 = \Gamma_0 + \Gamma_0^{ET}(c, \lambda_{exc}) + \Gamma_0^{ET \rightarrow SD}(c, \lambda_{exc}, t_d), \quad (9)$$

and

$$a = a_{PD} + a_{SD}(t_d) + a_{ET \rightarrow SD}(c, \lambda_{exc}, t_d), \quad (10)$$

In Eq. (9), the residual linewidth Γ'_0 is given by the sum of three terms: the fluorescence lifetime-limited value

$$\Gamma_0 = (2\pi\tau_{fl})^{-1} = 20 \text{ MHz}, \quad (11)$$

the direct energy transfer rate

$$\Gamma_0^{ET} \propto c^2, \quad (12)$$

which is consistent with a Förster radius $R_0 \approx 67$ Å, and the residual linewidth arising from “extra” SD triggered by ET

$$\Gamma_0^{ET \rightarrow SD} \propto c \log(t_d). \quad (13)$$

TABLE I. The six contributions to Γ'_{hom} as given by Eqs. (8)–(16), obtained at $\lambda_{exc} = 633$ nm and $t_d = 300$ s.

	$c = 1 \times 10^{-5}$ M	$c = 2 \times 10^{-3}$ M	$c = 6 \times 10^{-3}$ M
Γ_0 (MHz)	20	20	20
Γ_0^{ET} (MHz)	0	15	210
$\Gamma_0^{ET \rightarrow SD}$ (MHz)	0	350	1090
a_{PD} (MHz/K ^{1.3})	31	31	31
a_{SD} (MHz/K ^{1.3})	220	220	220
$a_{ET \rightarrow SD}$ (MHz/K ^{1.3})	0	80	170

In Eq. (10), the coupling constant a is also given by the sum of three terms: the “pure” dephasing contribution

$$a_{PD} = (31 \pm 10) \text{ MHz/K}^{1.3}, \quad (14)$$

which only depends on the guest-host coupling strength, the contribution of “normal” SD

$$a_{SD} \propto \log(t_d), \quad (15)$$

and the contribution of “extra” SD induced by ET

$$a_{ET \rightarrow SD} \propto c \log(t_d). \quad (16)$$

In Table I we have summarized the values obtained for the separate contributions to Γ'_0 and a , for three concentrations, in the blue wing ($\lambda_{exc} = 633$ nm) and for $t_d = 300$ s. The results have been cross-checked by a least-square fit of all available data (about 150 values of Γ'_{hom} for various concentrations, temperatures, delay times and excitation wavelengths) to the set of Eqs. (8)–(16).

Spectral diffusion induced by energy transfer proves to be a general phenomenon in doped organic glasses. It has by now also been observed for methyl-tetrahydrofuran and triethylamine doped with bacteriochlorophyll in hole-burning studies under high-pressure.^{12,20}

ACKNOWLEDGMENTS

We thank J. H. van der Waals for enlightening discussions. R.J.S. thanks the National Science Foundation for partial funding of this research and NWO for a visitor's grant to Leiden. The investigations were supported by the Netherlands Foundation for Physical Research (FOM) and Chemical Research (SON) with financial aid from the Netherlands Organization for Scientific Research (NWO).

¹J. M. A. Koedijk, T. M. H. Creemers, F. T. H. den Hartog, M. P. Bakker, and S. Völker, *J. Lumin.* **64**, 55 (1995); F. T. H. den Hartog, M. P. Bakker, J. M. A. Koedijk, T. M. H. Creemers, and S. Völker, *ibid.* **66&67**, 1 (1996).

²F. T. H. den Hartog, M. P. Bakker, R. J. Silbey, and S. Völker, *Chem. Phys. Lett.* (in press).

³S. Kulikov and J. P. Galaup, *J. Lumin.* **53**, 239 (1992).

⁴Y. V. Romanovskii, R. I. Personov, A. D. Samoilenko, K. Holliday, and U. P. Wild, *Chem. Phys. Lett.* **197**, 373 (1992).

⁵Th. Förster, *Ann. Phys. (Leipzig)* **2**, 55 (1948); in *Modern Quantum Chemistry, Part III*, edited by Sinanoglu (Academic, New York, 1965), p. 93.

⁶Th. Förster, *Z. Naturforsch. A* **4**, 321 (1949).

⁷M. Inokuti and F. Hirayama, *J. Chem. Phys.* **43**, 1978 (1965).

⁸A. Blumen and R. Silbey, *J. Chem. Phys.* **70**, 3707 (1978).

⁹S. Völker and R. M. Macfarlane, *J. Chem. Phys.* **73**, 4476 (1980).

¹⁰J. M. A. Koedijk, R. Wannemacher, R. J. Silbey, and S. Völker, *J. Phys. Chem.* **100**, 19945 (1996), and references therein.

- ¹¹R. Wannemacher, J. M. A. Koedijk, and S. Völker, *Chem. Phys. Lett.* **206**, 1 (1993).
- ¹²T. M. H. Creemers, J. M. A. Koedijk, I. Y. Chan, R. J. Silbey, and S. Völker, *J. Chem. Phys.* **107**, 4797 (1997).
- ¹³S. Völker, in *Relaxation Processes in Molecular Excited States*, edited by J. Fünfschilling (Kluwer, Dordrecht, 1989), pp. 113–242, and references therein; *Annu. Rev. Phys. Chem.* **40**, 499 (1989), and references therein.
- ¹⁴Optical Linewidths in Glasses, special issue of *J. Lumin.* **36**, 179 (1987), and references therein.
- ¹⁵R. J. Silbey, J. M. A. Koedijk, and S. Völker, *J. Chem. Phys.* **105**, 901 (1996).
- ¹⁶J. Black and B. I. Halperin, *Phys. Rev. B* **16**, 2879 (1977).
- ¹⁷P. Hu and L. R. Walker, *Solid State Commun.* **24**, 813 (1977); *Phys. Rev. B* **18**, 1300 (1978).
- ¹⁸R. Maynard, R. Rammal, and R. Suchail, *J. Phys. (France) Lett.* **41**, L-291 (1980).
- ¹⁹M. Pope and C. Swenberg, in *Electronic Processes in Organic Crystals* (Oxford University Press, Oxford, 1992), p. 100; G. Weber and F. J. W. Teale, *Discuss. Faraday Soc.* **27**, 134 (1959).
- ²⁰T. M. H. Creemers, A. J. Lock, and S. Völker (to be published).